

You may also like

Efficient time-symmetric simulation of torqued rigid bodies using Jacobi elliptic functions

To cite this article: E Celledoni and N Säfström 2006 *J. Phys. A: Math. Gen.* **39** 5463

View the [article online](#) for updates and enhancements.

- [Strong convergence of the vorticity and conservation of the energy for the -Euler equations](#)

Stefano Abbate, Gianluca Crippa and Stefano Spirito

- [Energy conservation in the limit of filtered solutions for the 2D Euler equations](#)

Takeshi Gotoda

- [On the conservation of energy in two-dimensional incompressible flows](#)

S Lanthaler, S Mishra and C Parés-Pulido

Efficient time-symmetric simulation of torqued rigid bodies using Jacobi elliptic functions

E Celledoni and N Säfström

Department of Mathematical Sciences, NTNU, Trondheim, Norway

Received 26 October 2005, in final form 26 January 2006

Published 24 April 2006

Online at stacks.iop.org/JPhysA/39/5463

Abstract

If the three moments of inertia are distinct, the solution to the Euler equations for the free rigid body is given in terms of Jacobi elliptic functions. Using the arithmetic–geometric mean algorithm (Abramowitz and Stegun 1992 *Handbook of Mathematical Functions with Formulas, Graphs, and Mathematical Tables* (New York: Dover)), these functions can be calculated efficiently and accurately. Compared to standard numerical ODE and Lie–Poisson solvers, the overall approach yields a faster and more accurate numerical solution to the Euler equations. This approach is designed for mass asymmetric rigid bodies. In the case of symmetric bodies, the exact solution is available in terms of trigonometric functions, see Dullweber *et al* (1997 *J. Chem. Phys.* **107** 5840–51), Reich (1996 *Fields Inst. Commun.* **10** 181–91) and Benettin *et al* (2001 *SIAM J. Sci. Comp.* **23** 1189–203) for details. In this paper, we consider the case of asymmetric rigid bodies subject to external forces. We consider a strategy similar to the symplectic splitting method proposed in Reich (1996 *Fields Inst. Commun.* **10** 181–91) and Dullweber *et al* (1997 *J. Chem. Phys.* **107** 5840–51). The method proposed here is time-symmetric. We decompose the vector field of our problem into a free rigid body (FRB) problem and another completely integrable vector field. The FRB problem consists of the Euler equations and a differential equation for the 3×3 orientation matrix. The Euler equations are integrated exactly while the matrix equation is approximated using a truncated Magnus series. In our experiments, we observe that the overall numerical solution benefits greatly from the very accurate solution of the Euler equations. We apply the method to the heavy top and the simulation of artificial satellite attitude dynamics.

PACS numbers: 02.60.Jh, 45.20.Jj

(Some figures in this article are in colour only in the electronic version)

1. Introduction

We consider the Euler equations describing the motion of a free (FRB) rigid body

$$I_1\dot{\omega}_1 = (I_2 - I_3)\omega_2\omega_3, \quad I_2\dot{\omega}_2 = (I_3 - I_1)\omega_3\omega_1, \quad I_3\dot{\omega}_3 = (I_1 - I_2)\omega_1\omega_2, \quad (1)$$

where I_1 , I_2 and I_3 are the principal moments of inertia. These equations are completely integrable. Energy and angular momentum are preserved along the solution; this means that for all times the two quantities

$$E = I_1\omega_1^2 + I_2\omega_2^2 + I_3\omega_3^2, \quad G^2 = I_1^2\omega_1^2 + I_2^2\omega_2^2 + I_3^2\omega_3^2 \quad (2)$$

are constant (here E is the energy and G^2 is the total angular momentum). There is also a non-canonical symplectic structure (Lie–Poisson structure) preserved by the flow of (1) [13]. By using the two constants of motion it is possible to derive the general solution of the equations expressed in terms of Jacobi elliptic functions.

The expression of the exact general solution of the Euler equations can be turned into a numerical method by using efficient numerical approximations of the Jacobi elliptic functions. To impose the initial conditions a constant τ , used to translate time, must be computed prior to the integration, see section 3 for details. In this paper, we show that this approach is very competitive and discuss the details of its further use in problems of rigid bodies subject to external forces. We also refer to [3, 16] for related literature.

The simulation of rigid body motion is interesting for applications in robotics, structural mechanics, molecular dynamics and also nanotechnology, [8, 10, 19]. Often stable integration over very long times is required in the simulations. It has been shown that the preservation of geometric features, as for example symplecticity and time symmetry of the flow for Hamiltonian systems, can be crucial for the performance of numerical integrators in long-time simulations [9, 10]. Therefore, in some cases geometric integrators are preferred to other existing sophisticated algorithms for multi-body systems.

Lie–Poisson integration methods for the Euler equations have been constructed by various authors [7, 12, 15, 17], see also [10] and references therein. Many of these methods cannot be straightforwardly generalized to the broader class of noncanonical Hamiltonian problems; thus their use is limited to the numerical approximation of the Euler equations. However, some of these integrators have successfully been applied in the simulation of rigid body dynamics and of torqued rigid bodies. This is for instance the case in [5, 18].

For the Euler equations, in [14, 18], the right-hand side of (1) is split into the following three terms:

$$f_1(\omega) = \begin{bmatrix} 0 \\ I_3\omega_3\omega_1 \\ -I_2\omega_1\omega_2 \end{bmatrix}, \quad f_2(\omega) = \begin{bmatrix} -I_3\omega_2\omega_3 \\ 0 \\ I_1\omega_1\omega_2 \end{bmatrix}, \quad f_3(\omega) = \begin{bmatrix} I_2\omega_2\omega_3 \\ -I_1\omega_3\omega_1 \\ 0 \end{bmatrix}. \quad (3)$$

Each of the three vector fields is Hamiltonian with respect to the rigid body Poisson bracket [13, p 8], and defines a differential equation which is easy to integrate exactly. The appropriate composition of the corresponding flows produces a (non-canonical) symplectic approximation of the problem. There is numerical evidence showing that this Lie–Poisson method is very competitive compared to most of the known and previously proposed integration strategies for the Euler equations [4, 14, 15]. We use this splitting for comparison in our numerical experiments. The generalization to the case of a six-dimensional system modelling torqued rigid bodies, in [18], is achieved by considering a splitting of the Hamiltonian of the problem in four parts, three of them give rise to vector fields analogous to f_1 , f_2 and f_3 , the last vector field is completely integrable and arises from the potential energy yielding the torque. We will briefly recall this approach in section 4.

The method proposed for torqued rigid bodies in the present paper is time-symmetric, and related to the approach of [5, 18]. We decompose the vector field of our problem into a FRB problem and another completely integrable vector field. The FRB problem is given by the three Euler equations and the differential equations for the orientation matrix. This matrix represents the rotation which the body undergoes with respect to a reference configuration. The numerical approximation of the Euler equations is performed to machine accuracy, while the orientation matrix is approximated by the exponential of a truncated Magnus series (achieving order 2 or 4). The overall splitting is symmetric, but not symplectic. However, in many of the considered numerical experiments the new method presents better conservation of energy and better behaviour of the numerical solution than the symplectic integrator of [5, 18].

Accurate approximations preserving energy, momentum and the Lie–Poisson structure of the Euler equations have been recently addressed in [15]. In this work, the authors propose a new implementation of the discrete Moser–Veselov (DMV) algorithm of [17]. By applying an appropriate rescaling of the initial condition, they also obtain new DMV methods of orders 4 and 6. The rescaling needs to be performed just once, at the beginning of the integration. The higher order methods present therefore virtually the same computational cost as the second-order DMV algorithm.

Our numerical tests show that using the exact solution and computing the Jacobi elliptic functions to machine accuracy leads to a very competitive method for the solution of the Euler equations, also compared to the improved DMV approach. Both approaches require the computation of some quantities prior to the time stepping, the rescaling factors for the DMV, and the constants for imposing the initial condition in the approach of Jacobi elliptic functions. This implies increased computational cost when the methods are used within a splitting technique for torqued rigid bodies. Our experiments show that the symmetric splitting method proposed in the present paper remains competitive also in the case of torqued rigid bodies.

The outline of the paper is as follows. The new method is presented in section 2. Some technical issues for the implementation of this approach are discussed in section 3. In section 4, we report some numerical experiments comparing the proposed approach to the DMV approach of [15] and the symplectic splitting of [5, 18].

2. A symmetric splitting method for torqued rigid bodies

Efficient integrators for the free rigid body can be used in connection with splitting methods in the numerical approximation of more complex rigid body dynamics. The method presented here can also be applied to problems of interacting rigid bodies, rigid body linked by constraints, etc [5, 18].

The Hamiltonian function for our problem is

$$\mathcal{H} = \mathcal{H}(\boldsymbol{\pi}, Q) = \frac{1}{2} \left(\frac{\pi_1^2}{I_1} + \frac{\pi_2^2}{I_2} + \frac{\pi_3^2}{I_3} \right) + V(Q),$$

where $\boldsymbol{\pi} = (I_1\omega_1, I_2\omega_2, I_3\omega_3)^T$ is the angular momentum and Q is the rotation matrix which describes the orientation of the body.

The Hamiltonian \mathcal{H} gives rise to the following system of ordinary differential equations,

$$\dot{\boldsymbol{\pi}} = \text{skew}(T^{-1}\boldsymbol{\pi})\boldsymbol{\pi} + f(Q), \quad (4)$$

$$\dot{Q} = \text{skew}(T^{-1}\boldsymbol{\pi})Q, \quad (5)$$

where

$$\text{skew}(\mathbf{v}) = \begin{pmatrix} 0 & v_3 & -v_2 \\ -v_3 & 0 & v_1 \\ v_2 & -v_1 & 0 \end{pmatrix},$$

f depends on the potential energy $V(Q)$ and

$$T = \begin{pmatrix} I_1 & 0 & 0 \\ 0 & I_2 & 0 \\ 0 & 0 & I_3 \end{pmatrix}$$

is the principal inertia tensor. To derive a symmetric splitting method for the above equations, we start by applying a Störmer/Verlet splitting,

$$\mathcal{H} = \mathcal{H}_1 + \mathcal{H}_2, \quad \mathcal{H}_2 = V(Q),$$

and $\mathcal{H}_1 = \mathcal{H} - \mathcal{H}_2$ is the kinetic energy. The system of differential equations is then split into the two systems,

$$S_1 = \begin{cases} \dot{\pi} = \text{skew}(T^{-1}\pi)\pi, \\ \dot{Q} = \text{skew}(T^{-1}\pi)Q, \end{cases} \quad (6)$$

corresponding to the kinetic part, and

$$S_2 = \begin{cases} \dot{\pi} = f(Q), \\ \dot{Q} = 0, \end{cases} \quad (7)$$

corresponding to the potential part. The Störmer/Verlet scheme is then

$$(\pi, Q)^{(j+1)} = \varphi_{h/2}^{[S_2]} \circ \varphi_h^{[S_1]} \circ \varphi_{h/2}^{[S_2]}((\pi, Q)^{(j)}), \quad j = 0, 1, \dots,$$

where $\varphi_h^{[S_1]}$ and $\varphi_h^{[S_2]}$ represent the exact flows of S_1 and S_2 , respectively. It is well known that this scheme is symplectic. In the case of symmetric rigid bodies, the exact flow $\varphi_h^{[S_1]}$ can be expressed in terms of trigonometric functions, see [2, 5, 18] for details. This is not true in the asymmetric case. Our splitting is obtained substituting $\varphi_h^{[S_1]}$ with a computationally efficient time-symmetric approximation of the flow of S_1 .

The system S_1 is simply a FRB problem. Rewriting the first part of system (6) in terms of the angular velocity, $\omega = T^{-1}\pi$ one obtains the Euler equations (1). We can now compute $\pi(t)$ to machine accuracy, for any t and any initial value, by using the exact solution of the Euler equations, and computing the Jacobi elliptic functions by the method of arithmetic–geometric mean, see section 3. Hence the update of π on the interval $[t_j, t_{j+1}]$ is

$$\pi^{(j+1)} = \mathcal{S}(\pi^{(j)}, h, t_j), \quad (8)$$

and is exact. The operator $\mathcal{S} : \mathbf{R}^3 \times \mathbf{R} \times \mathbf{R} \rightarrow \mathbf{R}^3$ maps any initial value $\pi(t_j) = \mathbf{v} \in \mathbf{R}^3$ to the solution, $\pi(t_{j+1}) = \mathcal{S}(\mathbf{v}, h, t_j)$, of the Euler equations at time $t_{j+1} = t_j + h$.

The approximation of the orientation matrix $Q^{(j+1)}$ in t_{j+1} is obtained integrating numerically on the interval $[t_j, t_{j+1}]$ the equation

$$\dot{Q} = \text{skew}(T^{-1}\pi)Q, \quad Q(t_j) = Q^{(j)},$$

using a symmetric Magnus method (of order 2 or 4) [9]. For order 2, this results in the following expression:

$$Q^{(j+1)} = \exp(h \text{ skew}(T^{-1}\pi^{(j+1/2)}))Q^{(j)}, \quad (9)$$

where $\pi^{(j+1/2)} = \pi(t_j + h/2)$ is obtained as a by-product of the update $\pi^{(j+1)}$ in (8) with little extra cost (see section 3 for details). The exponential in (9) is computed by Rodrigues formula

[13, p 291]. Thus, using (8) and (9), the flow $\varphi_h^{[S_1]}$ is approximated by a second-order flow $\phi_h^{[S_1]}$.

Given $f(Q^j)$ the flow $\varphi_h^{[S_2]}$ can be calculated exactly,

$$\pi^{(j+1)} = \pi^{(j)} + hf(Q^{(j)}), \quad Q^{(j+1)} = Q^{(j)},$$

and the updating (second-order) scheme is finally

$$(\pi^{(j+1)}, Q^{(j+1)}) = \varphi_{h/2}^{[S_2]} \circ \phi_h^{[S_1]} \circ \varphi_{h/2}^{[S_2]}((\pi^{(j)}, Q^{(j)})),$$

where

$$\phi_h^{[S_1]}((\pi^{(j)}, Q^{(j)})) = \begin{cases} \pi^{(j+1)} = \mathcal{S}(\pi^{(j)}, h, t_j), \\ Q^{(j+1)} = \exp(h \text{ skew}(T^{-1}\pi^{(j+1/2)}))Q^{(j)}, \end{cases} \quad (10)$$

$$\varphi_h^{[S_2]}((\pi^{(j)}, Q^{(j)})) = \begin{cases} \pi^{(j+1)} = \pi^{(j)} + hf(Q^{(j)}), \\ Q^{(j+1)} = Q^{(j)}. \end{cases} \quad (11)$$

It is easy to verify that $\phi_h^{[S_1]}\phi_{-h}^{[S_1]} = I$ and the overall splitting method has the time-symmetry property

$$\Phi_h \Phi_{-h} = 1, \quad \Phi_h = \varphi_{h/2}^{[S_2]} \circ \phi_h^{[S_1]} \circ \varphi_{h/2}^{[S_2]}.$$

Note that if we increase the number of terms included in the truncated Magnus series and obtain higher order in the approximation of $\varphi^{[S_1]}$, our scheme will accordingly be a more accurate approximation of the Störmer/Verlet splitting.

3. Implementation issues

Consider the values

$$\begin{aligned} a_1^2 &= 2EI_3 - G^2, & a_3^2 &= G^2 - 2EI_1, \\ b_1^2 &= I_2(I_3 - I_1), & b_3^2 &= I_2(I_2 - I_1), \end{aligned} \quad (12)$$

where G and E are given in (2) and I_1, I_2, I_3 are the principal moments of inertia in the Euler equations (1). Assume $b_3/a_3 \leq b_1/a_1$ (we will have a similar situation if $b_3/a_3 \geq b_1/a_1$), the solutions of the Euler equations are

$$\omega_1 = \frac{a_1 \operatorname{cn} u}{\sqrt{I_1(I_3 - I_1)}}, \quad \omega_2 = \frac{a_1 \operatorname{sn} u}{b_1}, \quad \omega_3 = \frac{a_3 \operatorname{dn} u}{\sqrt{I_3(I_3 - I_1)}}, \quad (13)$$

where cn , sn and dn are the Jacobi elliptic functions defined by

$$\operatorname{cn} u = \cos \varphi, \quad \operatorname{sn} u = \sin \varphi, \quad \operatorname{dn} u = \sqrt{1 - k^2 \sin^2 \varphi}, \quad (14)$$

with $u(t) = \lambda(t - \tau)$, $\lambda = b_1 a_3 / (I_2 \sqrt{I_1 I_3})$ and τ is a constant of integration. Here the amplitude φ is given implicitly as the solution of the equation

$$F(\varphi|k^2) = u(t), \quad u(t) = \lambda(t - \tau), \quad (15)$$

where

$$F(\varphi|k^2) := \int_0^\varphi \frac{d\theta}{\sqrt{1 - k^2 \sin^2 \theta}}$$

is an elliptic integral of the first kind with modulus $k = b_3 a_1 / (b_1 a_3)$. Assume $\omega^{(j)} = T^{-1}\pi^{(j)}$ is the approximation of the angular velocity produced by the symmetric splitting method at step j . At the next integration step we have to calculate the exact solution of the Euler equations, $\omega(t)$, at $t = t_j + h$ and $t = t_j + c_i h$, $c_i \in (0, 1)$, and $i = 1, \dots, s$, taking $\omega(t_j) = \omega^{(j)}$ as

an initial condition. In the case we integrate the equations for the orientation matrix with a Magnus method of order 2 we have $s = 1$ and $c_1 = 1/2$, and for order 4 we have $s = 2$, $c_{1,2} = 1/2 \pm \sqrt{3}/6$.

The first task of the process is to determine τ to satisfy the initial condition $\omega(t_j) = \omega^{(j)}$. To this end, we first find the amplitude $\varphi^{(j)} \in [0, 2\pi]$, which is uniquely determined from the equations

$$\omega_1(t_j) = \frac{a_1 \cos \varphi^{(j)}}{\sqrt{I_1(I_3 - I_1)}}, \quad \omega_2(t_j) = \frac{a_1 \sin \varphi^{(j)}}{b_1}.$$

Furthermore, from the sign of $\omega_3(t_j)$,

$$\omega_3(t_j) = \frac{a_3 \sqrt{1 - k^2 \sin^2 \varphi^{(j)}}}{\sqrt{I_3(I_3 - I_1)}},$$

we determine the sign of the constants a_3 and λ . Now from (15) we get

$$\tau = t_j - \frac{1}{\lambda} F(\varphi^{(j)} | k^2), \quad (16)$$

where

$$F(\varphi^{(j)} | k^2) = \int_0^{\varphi^{(j)}} \frac{d\theta}{\sqrt{1 - k^2 \sin^2 \theta}}. \quad (17)$$

The latter integral can be computed to the desired accuracy using the method of arithmetic–geometric mean of [1], briefly described below. We performed the numerical tests in MATLAB. To the best of our knowledge, there is no built-in routine in MATLAB evaluating the integral (17) for arbitrary values of $\varphi^{(j)}$. The procedure we implemented is analogous to that used in the MATLAB function `ellipke` for computing the complete elliptic integrals of the first kind ($F(\pi/2 | k^2)$).

Consider the sequence $\{\varphi_n^{(j)}\}_{n=0,1,\dots}$, $\varphi_{n+1}^{(j)} > \varphi_n^{(j)}$ defined by

$$\tan(\varphi_{n+1} - \varphi_n) = \frac{b_n}{a_n} \tan \varphi_n, \quad \varphi_0 = \varphi^{(j)},$$

where a_n, b_n are given by the arithmetic–geometric mean sequence [1], i.e.

$$a_{n+1} = \frac{a_n + b_n}{2}, \quad b_{n+1} = \sqrt{a_n b_n}, \quad c_{n+1} = \frac{a_n - b_n}{2}. \quad (18)$$

Taking the initial values

$$a_0 = 1, \quad b_0 = \sqrt{1 - k^2}, \quad c_0 = k,$$

one can show that

$$F(\varphi_0 | k^2) = \lim_{n \rightarrow \infty} \frac{\varphi_n}{2^n a_n}, \quad \varphi_0 = \varphi^{(j)}. \quad (19)$$

The iteration stops when $n = N$ and c_N in (18) is less than tolerated error. As the arithmetic–geometric mean sequence, (18), converges quadratically, one obtains accurate approximations of $F(\varphi^{(j)} | k^2)$ in very few recursion steps. In our implementation we terminate the iteration when c_N is less than machine epsilon.

From (16) we easily obtain τ . At this point to find the solution of the Euler equations at the desired time values we can use the built-in MATLAB function `ellipj`, with input

$$[\lambda(t_j + c_1 h - \tau), \dots, \lambda(t_j + c_s h - \tau), \lambda(t_{j+1} - \tau)]^T.$$

We obtain in output the corresponding values of cn , sn , dn and after appropriate rescaling (13), we obtain the values of the solution at $t_j + c_1 h, \dots, t_j + c_s h, t_{j+1}$.

The MATLAB function `ellipj` is based on a similar algorithm as that described above. In our implementation we reuse the arithmetic–geometric mean sequence obtained in the computation of τ .

Note that φ , from relation (17), can be found explicitly for the special case $k^2 = 1$ or $k^2 = 0$.

4. Numerical experiments

The second-order symmetric splitting method proposed in this paper is denoted in the following by SEJ and compared with the symplectic method of [5, 18] which we denote in short by MR. We denote with SEJ4 the second-order symmetric splitting method where the Magnus method of order 4 in the integration of (6) is used. The approach for solving the Euler equations is also compared with the discrete Moser–Veselov methods of [15] (DMV). The symplectic method MR is based on a splitting of the Hamiltonian \mathcal{H} into four parts:

$$\tilde{\mathcal{H}}_1 = \frac{\pi_1^2}{2I_1}, \quad \tilde{\mathcal{H}}_2 = \frac{\pi_2^2}{2I_2}, \quad \tilde{\mathcal{H}}_3 = \frac{\pi_3^2}{2I_3}, \quad \tilde{\mathcal{H}}_4 = V(Q).$$

Each of the corresponding Hamiltonian vector fields can be integrated exactly ($\tilde{\mathcal{H}}_1, \tilde{\mathcal{H}}_2, \tilde{\mathcal{H}}_3$ correspond to the vector fields (3)), the symmetric composition of the flows gives rise to the approximation scheme

$$(\pi, Q)^{(j+1)} = \Phi_M((\pi, Q)^{(j)}),$$

where

$$\Phi_M = \varphi_{4,h/2} \circ \Phi_{T,h} \circ \varphi_{4,h/2}.$$

Here

$$\Phi_{T,h} = \varphi_{1,h/2} \circ \varphi_{2,h/2} \circ \varphi_{3,h} \circ \varphi_{2,h/2} \circ \varphi_{1,h/2}$$

is the contribution from the kinetic parts, $\tilde{\mathcal{H}}_1, \tilde{\mathcal{H}}_2$ and $\tilde{\mathcal{H}}_3$. The flows of the kinetic parts correspond to elementary rotations in \mathbf{R}^3 . For example for $\tilde{\mathcal{H}}_1$,

$$\varphi_{1,h}((\pi, Q)^{(j)}) = \begin{cases} \pi^{(j+1)} = R_x(h)\pi^{(j)}, \\ Q^{(j+1)} = R_x(h)Q^{(j)}, \end{cases}$$

where

$$R_x(h) = \begin{pmatrix} 1 & 0 & 0 \\ 0 & \cos(C^{(j)}h) & \sin(C^{(j)}h) \\ 0 & -\sin(C^{(j)}h) & \cos(C^{(j)}h) \end{pmatrix},$$

and

$$C^{(j)} = \frac{\pi_1^{(j)}}{I_1}.$$

while the flow for $\tilde{\mathcal{H}}_4$ is the same as for the system S_2 (5) of the previous section, i.e. $\varphi_{4,h} = \varphi_h^{[S_2]}$.

4.1. Free rigid body experiments

In the first experiment we consider the integration of Euler’s equations. In this experiment we perform a comparison of the use of `ellipj` in MATLAB for computing the exact solution of the equations (approach here denoted with JE in the figures) with the MR and DMV methods. We refer to [15, 17] for a detailed description of the DMV methods, and recall that the higher order

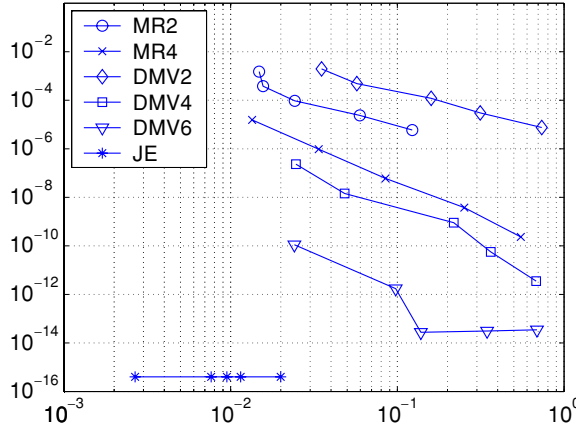


Figure 1. Euler's equations. Execution times (x -axis) against the norm of the global error at $t = 1$ (y -axis). Integration on the interval $[0, 1]$ with different step sizes. The methods are MR of orders 2 and 4, DMV of orders 2, 4 and 6, and the method JE based on the accurate computation of the Jacobi elliptic functions using ellipj in MATLAB. The results are the average over 200 experiments. The initial condition is $\pi_0 = [-1, 0, 2]^T$. The principal moments of inertia are $I_1 = 5, I_2 = 4, I_3 = 3$.

DVM are obtained by computing an appropriate rescaling of the initial condition. In figure 1 we plot on the x -axis the execution times employed by the methods to perform the integration on the interval $[0, 1]$, for different choices of the step size, $h = 1/(2^k)$ and $k = 2, \dots, 6$. On the y -axis we report the corresponding values of the 2-norm of the global error. In all the experiments the reference solution for computing the global error is obtained using the built-in function of MATLAB, `ode45`, setting the absolute and relative tolerance equal to 10^{-14} . The MR method in this case involves the computation of the three flows corresponding to the Hamiltonians $\tilde{\mathcal{H}}_1, \tilde{\mathcal{H}}_2, \tilde{\mathcal{H}}_3$ only.

The JE approach produces, as expected, a very accurate solution of the problem, the error is of the size of 10^{-14} and is independent of the step size of integration. The MR and DMV methods of orders 2 and 4 perform similarly with a slight advantage for the MR in the second-order case, and of DVM in the fourth-order case.

The execution times are computed taking an average over 200 experiments. In this experiment the principal moments of inertia and the initial value are $I_1 = 5, I_2 = 4, I_3 = 3$ and $\pi_0 = (1, 0, 2)^T$. The cost for computing the rescaling factors in the DMV methods and for the computation of τ in JE are not included in this experiment. The excellent performance of the JE approach, compared to the other considered methods, shows that the arithmetic–geometric mean algorithm is a very efficient method for the evaluation of the Jacobi elliptic functions.

We repeated this experiment, on the interval $[0, 400]$ with step size $h = 0.4$, and considered the energy error as the difference between the constant exact energy, given by \mathcal{H} , and the energy obtained from the numerical methods. For the MR method of orders 2 and 4 the energy error is oscillating near zero (the amplitude of the oscillations is about 10^{-3} for order 2, and about 10^{-5} for the method of order 4). The DMV methods give an energy error of the size of 10^{-13} , and for the JE approach the energy is about 10^{-16} .

In the second experiment we consider the integration of the FRB problem (6). In figure 2 we report the execution times (x -axis) against the norm of the global error at $t = 1$ (y -axis). The integration is performed on the interval $[0, 1]$ with different step sizes. We denote with

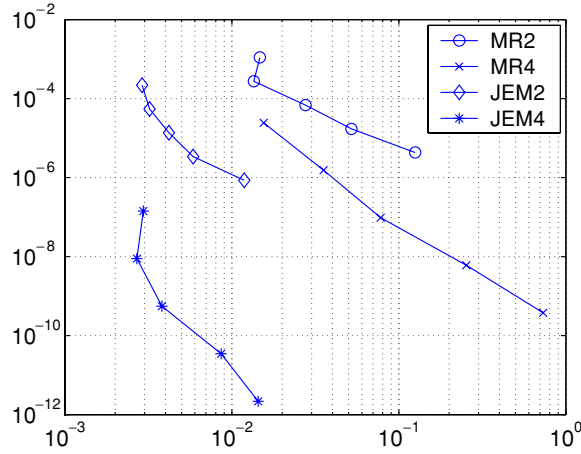


Figure 2. FRB equations (6). Execution times (x-axis) against the norm of the global error at $t = 1$ (y-axis). Integration on the interval $[0, 1]$ with different step sizes. The considered methods are MR of orders 2 (MR2) and 4 (MR4), and the methods JEM2 and JEM4 (combination of `ellipj` in MATLAB with a Magnus method of order 2 or 4). The results are the average over 200 experiments. The initial conditions are $\pi_0 = [-1, 0, 2]^T$, and Q_0 is equal to the 3×3 identity matrix. The principal moments of inertia are $I_1 = 5$, $I_2 = 4$, $I_3 = 3$.

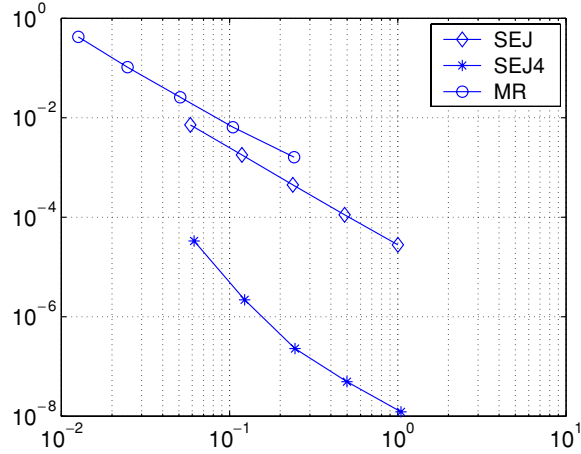


Figure 3. Heavy top. Execution times (x-axis) against the norm of the global error at $t = 1$ (y-axis). Integration on the interval $[0, 1]$ with different step sizes. The results are the average over 200 experiments. We consider the symmetric splitting methods SEJ and SEJ4 and the symplectic splitting MR. All the methods have order 2. The initial conditions are $\omega_0 = [10, 10, 10]^T$, $u_0 = [0, 0, 1]^T$. The principal moments of inertia are $I_1 = 1000$, $I_2 = 5000$, $I_3 = 6000$.

JEM2 or JEM4 the methods based on the use of `ellipj` in MATLAB (for the solution of Euler's equations), combined with a Magnus method for the computation of the orientation matrix (Magnus method of order 2 (JEM2) and order 4 (JEM4), see section 2). The comparison is made with the MR methods of orders 2 and 4. The results are given as an average over 200 repeated experiments. The initial conditions are $\pi_0 = [-1, 0, 2]^T$, Q_0 is equal to the 3×3 identity matrix, and $I_1 = 5$, $I_2 = 4$, $I_3 = 3$. Also in this case the JEM methods perform very well.

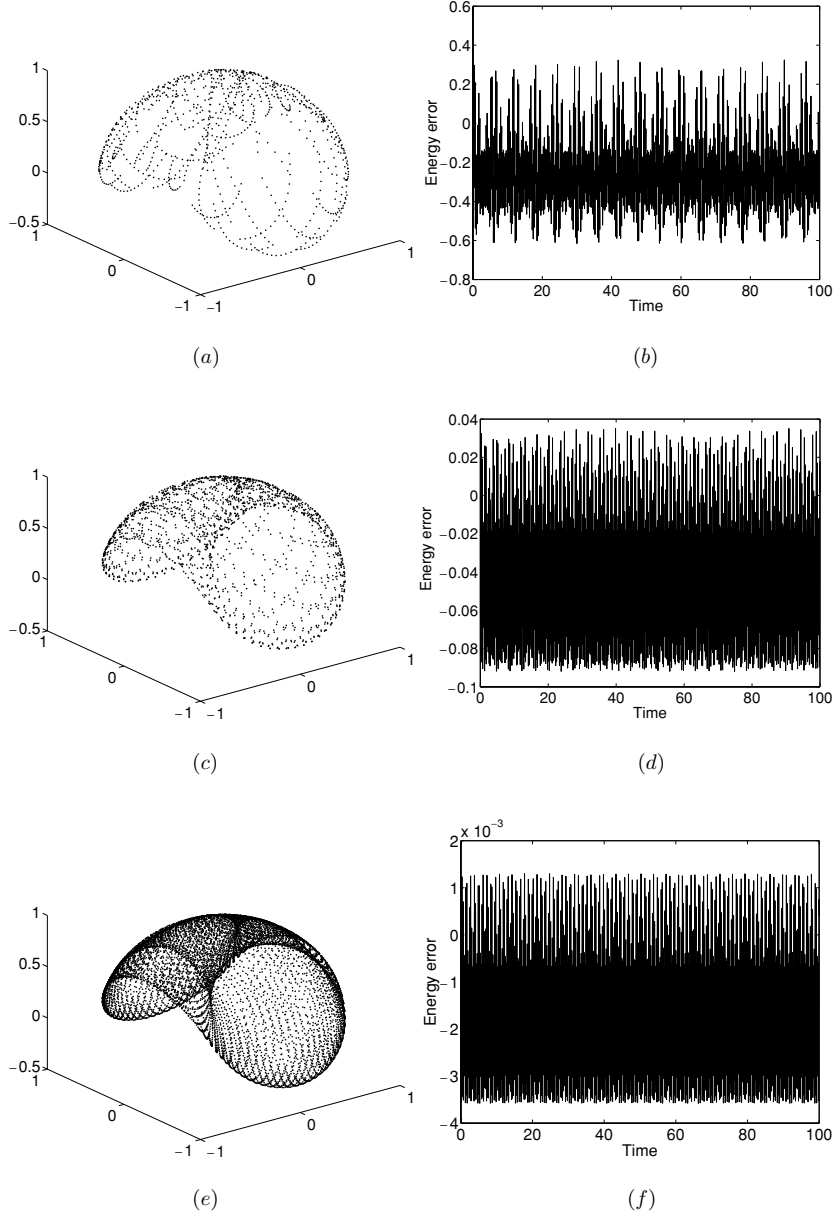


Figure 4. Energy error for the heavy top. Integration on the interval $[0, 100]$, using the method SEJ. $I_1 = 1000$, $I_2 = 5000$, $I_3 = 6000$, $\omega_0 = [10, 10, 10]^T$. (a) Centre of mass u , $h = 0.1$, SEJ. (b) SEJ, $h = 0.1$. (c) Centre of mass u , $h = 0.05$, SEJ. (d) SEJ, $h = 0.05$. (e) Centre of mass u , $h = 0.01$, SEJ. (f) SEJ, $h = 0.01$.

4.2. Heavy top experiments

In figure 3 we report the results of the third experiment. We consider the integration of the heavy top problem which corresponds to taking

$$V(Q) = e_3^T Q u_0,$$

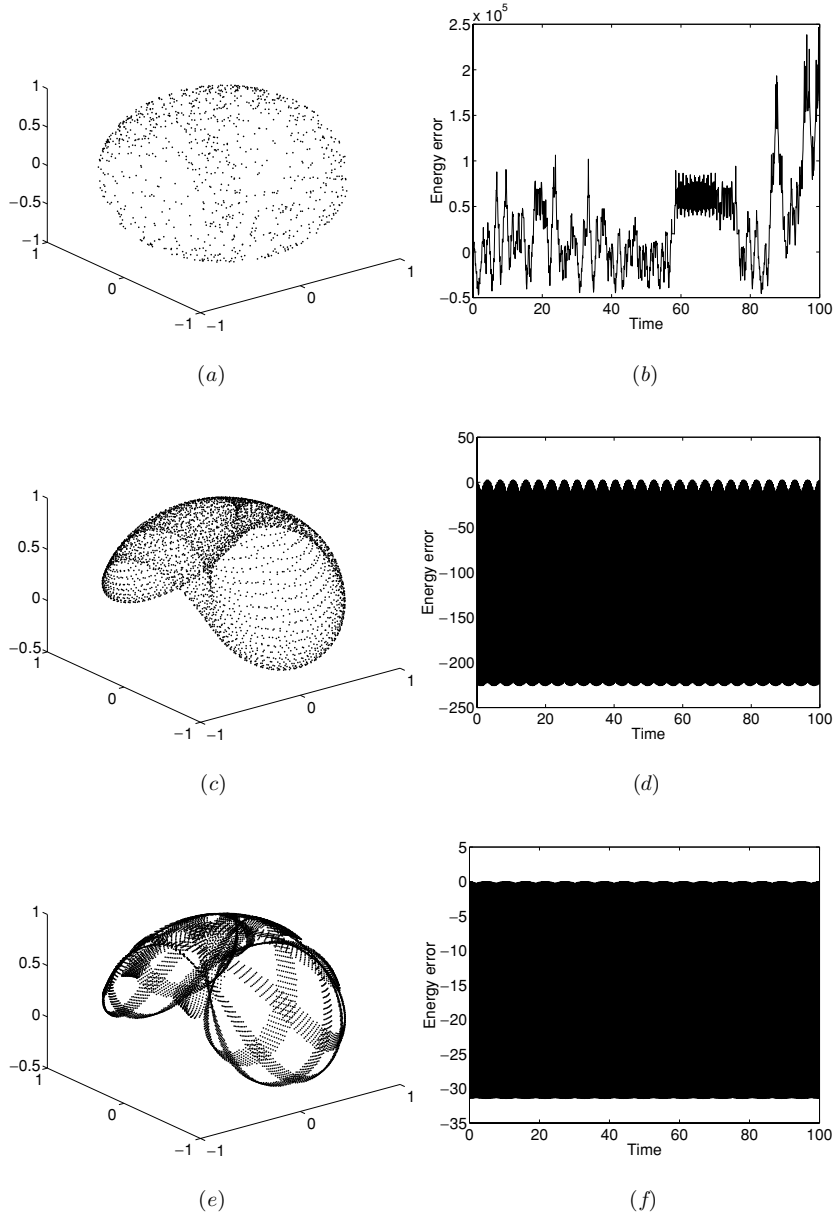


Figure 5. Energy error for the heavy top. Integration on the interval $[0, 100]$, using the method MR. $I_1 = 1000, I_2 = 5000, I_3 = 6000, \omega_0 = [10, 10, 10]^T$. (a) Centre of mass $u, h = 0.1$, MR. (b) MR, $h = 0.1$. (c) Centre of mass $u, h = 0.05$, MR. (d) MR, $h = 0.05$. (e) Centre of mass $u, h = 0.01$, MR. (f) MR, $h = 0.01$.

where e_3 is the third canonical vector and u_0 is the initial position of the centre of mass of the heavy top. This gives rise to a torque in (4) of the form

$$f(Q) = \begin{bmatrix} u_2 \\ -u_1 \\ 0 \end{bmatrix}, \quad \mathbf{u}(t) = Q(t)\mathbf{u}_0.$$

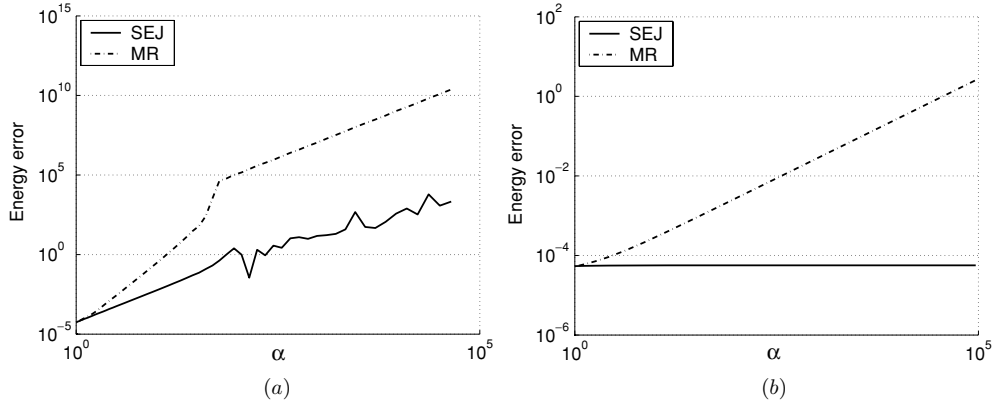


Figure 6. Energy error for the heavy top, $u_0 = [0, 0, 1]^T$. Integration on the interval $[0, 10]$, $h = 0.01$. In (a) we vary the initial angular velocity, $\omega_0 = \alpha[1, 2, 3]^T$, and let $I_1 = 1$, $I_2 = 2$, $I_3 = 3$ be fixed. In (b) we vary the principal moments of inertia, $I_1 = \alpha$, $I_2 = 2\alpha$, $I_3 = 3\alpha$, and let $\omega_0 = [1, 2, 3]^T$ be fixed.

We use the second-order splitting methods MR and SEJ and SEJ4 on the interval $[0, 1]$. The principal moments of inertia are $I_1 = 1000$, $I_2 = 5000$, $I_3 = 6000$, and the initial conditions are $\omega_0 = (10, 10, 10)^T$ and $u_0 = (0, 0, 1)^T$.

We first integrate on the interval $[0, 1]$ and compare the performance of the two splitting methods in terms of execution times against the norm of the global error, figure 3. In this case the advantage of the SEJ4 splitting method is quite clear while MR and SEJ perform similarly.

Next we illustrate the qualitative performance of the two methods SEJ and MR. We look at the energy error and at the numerical trajectory describing the motion of the centre of mass, integrating on the time interval $[0, 100]$. The results are shown in figures 4 and 5. We compare the results obtained by using different step sizes for MR and SEJ. For small step sizes we expect the methods to produce similar trajectories. We would like the methods to reproduce the correct qualitative behaviour of the solution also for bigger step sizes. For step size $h = 0.01$, figures 4(f) and 5(f), the two methods produce trajectories such that

$$\frac{1}{N} \sum_{n=1}^N \|u_{SEJ,n} - u_{MR,n}\| = \mathcal{O}(10^{-1}),$$

and $N = 100/0.01$ is the total number of steps. The energy error for SEJ is a factor 10^{-4} smaller than for MR. Increasing the step size to $h = 0.05$ and $h = 0.1$, the amplitude of the oscillations in the energy error increases for both methods. Consistently for all the experiments, SEJ has a much smaller energy error than MR, figures 4(b), (d) and (f), 5(b), (d) and (f). For step size $h = 0.1$ the trajectory of the centre of mass produced by the MR method is different from the one produced with a step size $h = 0.01$, figures 5(a) and (e). For the SEJ method the numerical trajectory of the centre of mass maintains the same character for the different step sizes $h = 0.01$, $h = 0.05$ and $h = 0.1$, figures 4(a), (c) and (e).

Next, we compare the energy error between the two methods for different values of the angular velocity, figure 6(a), and the inertia tensor, figure 6(b). The initial position of the centre of mass is $u_0 = (0, 0, 1)$. We consider the time interval $[0, 10]$ and integrate with a

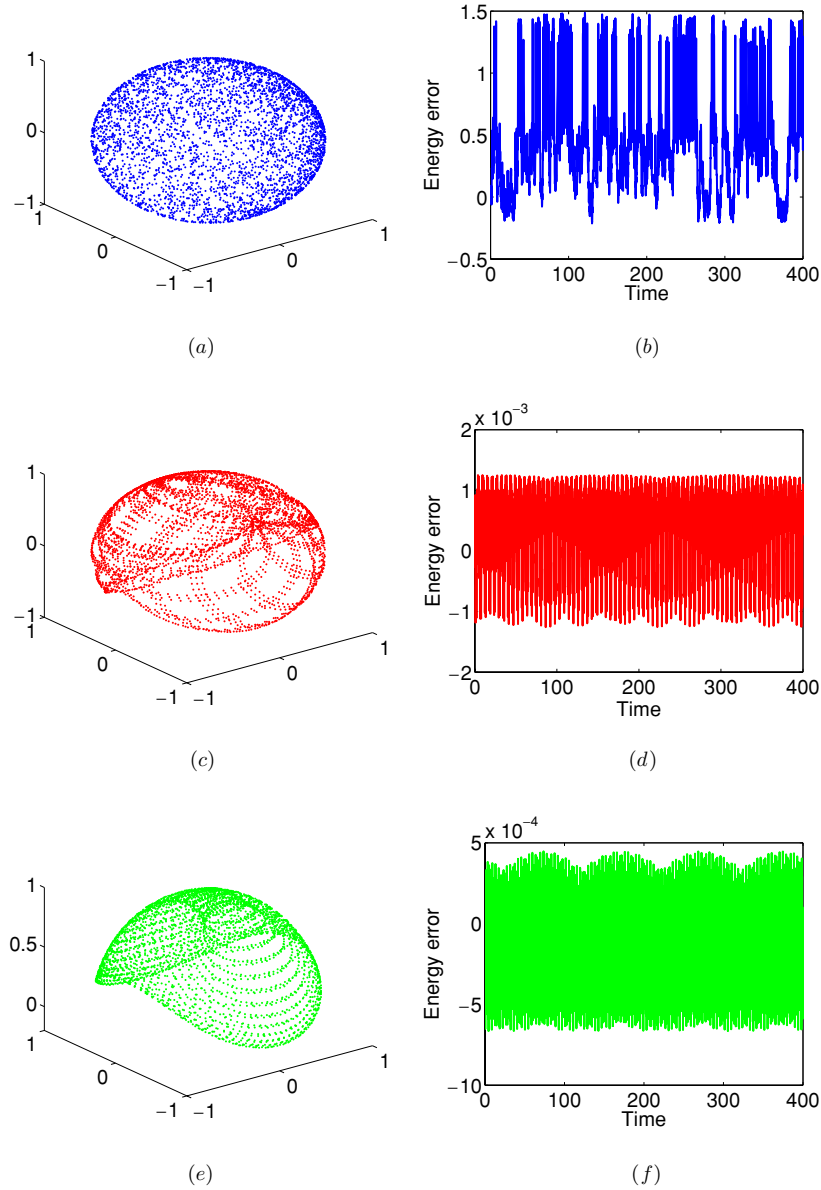


Figure 7. Plot of Qe_3 and the relative energy error for the satellite simulation. Integration on the interval $[0, 400]$ with $h = 0.1$, using the methods MR, SEJ and SEJ4 (SEJ with a Magnus method of order 4 for the rotation matrix Q). The principal moments of inertia are $I_1 = 1.7 \times 10^4$, $I_2 = 3.7 \times 10^4$, $I_3 = 5.4 \times 10^4$. The initial angular velocity is $\omega_0 = [15, -15, 15]^T$ and $Q(0)$ is the 3×3 identity matrix. (a) Body frame Qe_3 , $h = 0.1$, MR. (b) Relative energy error MR, $h = 0.1$. (c) Body frame Qe_3 , $h = 0.1$, SEJ. (d) Relative energy error SEJ, $h = 0.1$. (e) Body frame Qe_3 , $h = 0.1$, SEJ4. (f) Relative energy error SEJ4, $h = 0.1$.

step size $h = 0.01$. In figure 6 we report on the y-axis the average absolute value of the energy error

$$\frac{1}{N} \sum_{n=1}^N |\mathcal{H} - \mathcal{H}_n|,$$

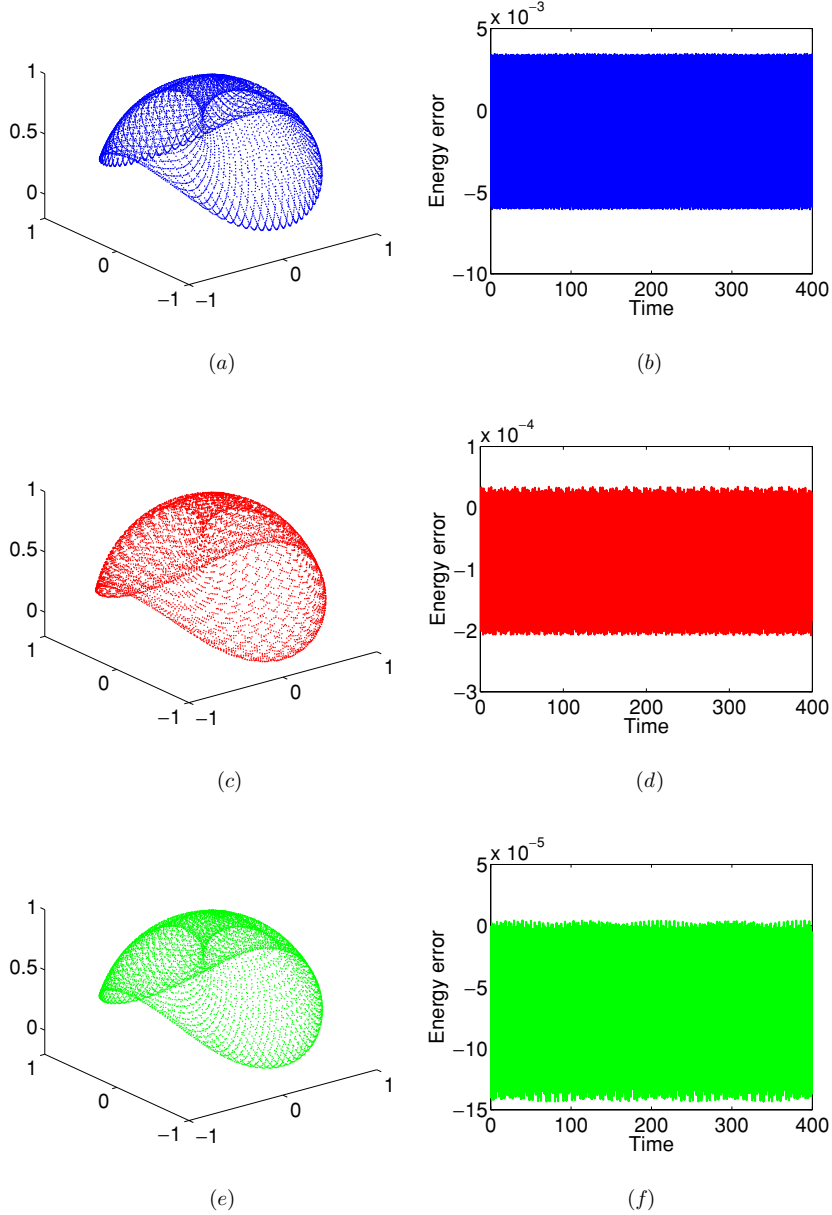


Figure 8. Plot of Qe_3 and the relative energy error for the satellite simulation. Integration on the interval $[0, 400]$, using the methods MR, SEJ and SEJ4 (SEJ with a Magnus method of order 4 for the rotation matrix Q). The principal moments of inertia are $I_1 = 1.7 \times 10^4$, $I_2 = 3.7 \times 10^4$, $I_3 = 5.4 \times 10^4$. The initial angular velocity is $\omega_0 = [15, -15, 15]^T$ and $Q(0)$ is the 3×3 identity matrix. (a) Body frame Qe_3 , $h = 0.05$, MR. (b) Relative energy error MR, $h = 0.05$. (c) Body frame Qe_3 , $h = 0.05$, SEJ. (d) Relative energy error SEJ, $h = 0.05$. (e) Body frame Qe_3 , $h = 0.05$, SEJ4. (f) Relative energy error SEJ4, $h = 0.05$.

with \mathcal{H}_n the value of the numerical energy for the methods at time step n and \mathcal{H} the exact energy value, and $N = 10/0.01 = 1000$. On the x -axis we report the value of a parameter α used for varying the initial angular velocity $\omega_0 = \alpha[1, 2, 3]^T$, with fixed principal moments of

inertia $I_1 = 1$, $I_2 = 2$, $I_3 = 3$, figure 6(a). In figure 6(b) α is instead used to vary the principal moments of inertia $I_1 = \alpha$, $I_2 = 2\alpha$, $I_3 = 3\alpha$ while keeping $\omega_0 = [1, 2, 3]^T$ fixed. From the two plots in figure 6 it appears that the energy error for the SEJ method is smaller compared to the MR method in some cases. This happens when the angular velocity or inertia is large, i.e. when the external torque is relatively small compared to the momentum.

4.3. Satellite experiments

Assume μ and r are given constants and the potential energy is given by

$$V(Q) = 3 \frac{\mu}{2r^3} (Qe_3)^T T Q e_3,$$

where T is the inertia tensor and Qe_3 is the third column of Q . The torque $f(Q)$ in equation (5) is here given by

$$f(Q) = 3 \frac{\mu}{r^3} (Qe_3) \times (T Q e_3).$$

This test problem is a simplified version of the model describing the motion of a satellite in a circular orbit of radius r around the earth, [11]. In our test problem the energy is preserved. We take $\mu = GM$ where G is the gravitational constant and M is the mass of the earth.

Recall that we indicate with SEJ4 the second-order symmetric splitting method where the rotation matrix Q is approximated with a Magnus method of order 4, while for the SEJ method the rotation matrix Q is approximated with a second-order Magnus method as in (9).

In the first experiment on the satellite model we compare the methods MR, SEJ and SEJ4. The inertia moments are chosen to be

$$I_1 = 1.7 \times 10^4, \quad I_2 = 3.7 \times 10^4, \quad I_3 = 5.4 \times 10^4,$$

the initial condition for the angular velocity is

$$\omega_0 = [15, -15, 15]^T,$$

and $Q(0) = I$ (the identity matrix). Similar values are considered for tests performed in [16]. We have $\mu = GM = 3.986 \times 10^{14}$, $r = 1.5 \times 10^5$. We integrate on the interval $[0, 400]$ for two different step sizes $h = 0.1$ and $h = 0.05$. In figure 7, the step size is $h = 0.1$. Figures 7(a), (c) and (e) in the left column show the trajectory described by the vector Qe_3 . The method SEJ4 gives the best results.

In the right column of figure 7, the energy error for the three methods is presented. Both SEJ and SEJ4 preserve the energy much better than the MR method.

In figure 8, the step size is $h = 0.05$. Here the three different methods perform similarly. Also in this case the SEJ methods give better energy preservation compared to MR.

In some of the presented experiments we have considered different orderings of the elementary flows which define the MR methods, this has not given significant differences in the results. An analysis of how different compositions of the flows can influence the size of the energy error can be found in [6]. We do not exclude that appropriate orderings of the flows can give improved performance for the MR splitting in some cases.

5. Conclusions

In this paper we presented a symmetric splitting method for the integration of rigid body problems subject to external forces. The numerical strategy is based on the use of available efficient algorithms for the computation of Jacobi elliptic functions. We compared the method with a similar symplectic splitting method of [18] and [5]. In many of the performed

experiments the presented symmetric splitting is more efficient than the symplectic splitting. Moreover, the new method presents in many experiments a better energy conservation. This happens especially for problems where the principal moments of inertia are of large size.

Acknowledgments

The authors are grateful to Brynjulf Owren and Robert McLachlan for promoting the use of the exact solution of the Euler equations in numerical integrators, to Antonella Zanna for useful discussions, and for providing the codes with the implementation of the discrete Moser–Veselov algorithms of [15], and to the anonymous referee for very useful comments.

References

- [1] Abramowitz M and Stegun I A 1992 *Handbook of Mathematical Functions with Formulas, Graphs, and Mathematical Tables* (National Bureau of Standards Applied Mathematics Series vol 55) (New York: Dover) (reprint of the 1972 edn)
- [2] Benettin G, Cherubini A M and Fassò F 2001 A changing-chart symplectic algorithm for rigid bodies and other hamiltonian systems on manifolds *SIAM J. Sci. Comput.* **23** 1189–203
- [3] Butcher J 2003 *Numerical Methods for Ordinary Differential Equations* 2nd edn (New York: Wiley)
- [4] Celledoni E and Owren B 2003 Lie group methods for rigid body dynamics and time integration on manifolds *Comput. Methods Appl. Mech. Eng.* **192** 421–38
- [5] Dullweber A, Leimkuhler B and McLachlan R 1997 Symplectic splitting methods for rigid body molecular dynamics *J. Chem. Phys.* **107** 5840–51
- [6] Fassò F 2003 Comparison of splitting algorithms for the rigid body *J. Comput. Phys.* **189** 527–38
- [7] Ge Z and Marsden J E 1988 Lie–Poisson Hamilton–Jacobi theory and Lie–Poisson integrators *Phys. Lett. A* **133** 134–9
- [8] Geradin M and Cardona A 2001 *Flexible Multibody Dynamics* (New York: Wiley)
- [9] Hairer E, Lubich C and Wanner G 2002 *Geometric Numerical Integration* (*Springer Series in Computational Mathematics* vol 31) (Berlin: Springer)
- [10] Leimkuhler B and Reich S 2004 *Simulating Hamiltonian Dynamics* (*Cambridge Monographs on Applied and Computational Mathematics* vol 14) 1st edn (Cambridge: Cambridge University Press)
- [11] Leok M, Lee T and McClamroch N H 2005 Attitude maneuvers of a rigid spacecraft in a circular orbit *Proc. Am. Control Conf.* to appear
- [12] Lewis D and Simo J C 1994 Conserving algorithms for the dynamics of Hamiltonian systems of Lie groups *J. Nonlinear Sci.* **4** 253–99
- [13] Marsden J E and Ratiu T S 1994 *Introduction to Mechanics and Symmetry* (Berlin: Springer)
- [14] McLachlan R I 1993 Explicit Lie–Poisson integration and the Euler equations *Phys. Rev. Lett.* **71** 3043–6
- [15] McLachlan R I and Zanna A 2005 The discrete Moser–Veselov algorithm for the free rigid body, revisited *Found. Comput. Math.* **5** 87–123
- [16] Mitchell J Wm 2000 A simplified variation of parameters solution for the motion of an arbitrarily torqued mass asymmetric rigid body *PhD Thesis* University of Cincinnati
- [17] Moser J and Veselov A 1991 Discrete versions of some classical integrable systems and factorization of matrix polynomials *J. Commun. Math. Phys.* **139** 217–43
- [18] Reich S 1996 Symplectic integrators for systems of rigid bodies. Integration algorithms and classical mechanics (Toronto, ON, 1993) *Fields Inst. Commun.* **10** 181–91
- [19] Sohlberg K, Tuzunand R E, Sumpter G and Noid D W 1997 Application of rigid-body dynamics and semiclassical mechanics to molecular bearings *Nanotechnology* **8** 103–11